



# Low-lying $Pt_n$ cluster structures ( $n = 6–10$ ) from global optimizations based on DFT potential energy surfaces: Sensitivity of the chemical ordering with the functional



Rui Li, Marc Odunlami, Philippe Carbonnière\*

IPREM/ECP, UMR CNRS 5254, Groupe de Chimie Théorique Université de Pau et des Pays de l'Adour, Hélioparc Pau-Pyrénées, 2 Avenue du président Angot, 64053 Pau Cedex 9, France

## ARTICLE INFO

### Article history:

Received 18 November 2016

Received in revised form 10 February 2017

Accepted 10 February 2017

Available online 17 February 2017

### Keywords:

Pt clusters

DFT methods

Global optimization

Low-lying structures

## ABSTRACT

Through the example of the small  $Pt_6$  clusters the low-lying structures and their chemical ordering obtained with the four classes of functionals: GGA (PBE), hybrid GGA (PBE0), meta-GGA (TPSS) and hybrid meta-GGA (TPSSH), were investigated with the cc-pVTZpp basis set. Moreover, the spin multiplicities from singlet to nonet were considered. The results yield two different pictures: singlet to septet planar structures are favored with the pure functionals while quintet to nonet 3D structures appear as the lowest energy structures or first isomers for their hybrid counterpart. Qualitative trends obtained from RMP4(SDQ) calculations suggest a more correct description at the DFT level by the use of hybrid functionals. The investigation of the lowest energy structures of  $Pt_{7–10}$  clusters at the TPSSH level in comparison with the GGA picture issuing from the literature confirm the preference for 3D compact structures. This highlights a different morphological map of the small  $Pt_n$  clusters and suggests a clearer pattern growth from  $Pt_6$  toward the lowest energy  $Pt_{10}$  structure.

© 2017 Elsevier B.V. All rights reserved.

## 1. Introduction

(Sub-)nanometer sized metal cluster consists of only several atoms to several tens of atoms. Due to its small size and quantum effects, it could have very specific electronic, optical, magnetic and catalytic properties comparing with their bulk behaviors [1,2]. The number of stable structures of atomic nanocluster grows exponentially with its size. These most stable structures called as low-lying isomers (or conformers in the case of molecular clusters) are located by the exploration of the potential energy surface (PES) of the system, which is also called as energy landscape. The PES corresponds to the molecular energy of the nanocluster system with respect to their nuclear parameters. By analogy, the PES can be compared in the 3D space to a landscape formed by mountains, hills and valleys. The “valleys” in the PES represents the local minima of energy, and the lowest of them is called global minimum. Each minimum on the PES corresponds to a set of coordinates for which the system is considered as stable.

“Global optimizations” (GO) were proposed to locate the relevant local minima and covered by several reviews (see for instance Refs. [3–6] and therein). The first class of methods is based on thermodynamics principles in which the temperature of the system is

introduced to guide the morphological evolution of the nanocluster toward the global minimum. This is the case of the methods based on Molecular Dynamics (MD) [7] and Monte Carlo (MC) [8] approaches: the system can be cooling down at different steps of its morphological evolution to locate the global minimum (Simulated Annealing [9]) or several trajectories from random structures can be carried out simultaneously at different temperatures followed by exchange moves between configurations (Parallel Tempering [10]). The second class of global optimization methods, highly parallelizable by essence, consists in several local optimizations of selected structures from evolutionary principles: For instance, the genetic algorithm (GA) [11] starts from a small set of initial structures which are firstly optimized (parents) and from which an additional set of structures (children) is generated from mating and mutating operations. After re-optimization, the lowest energy structures are considered for the next iteration (generation) until the convergence of the low-lying structures. The Basin Hopping algorithm (BH) [12,13] can be used as a variant of the first or the second class of algorithm since it uses random hopping moves combined to local minimizations to jump from one minimum of the PES to another.

Concerning the computations of the energy (or the forces) of the system, empirical force fields such as Coulomb-Born-Mayer [14], Lennard-Jones [15], Morse [16], Z potential [17], and more specifically for metallic species Sutton-Chen [18] and GUPTA [19]

\* Corresponding author.

E-mail address: [philippe.carbonniere@univ-pau.fr](mailto:philippe.carbonniere@univ-pau.fr) (P. Carbonnière).

potentials are widely used. On one side it allows an extremely fast exploration of the PES and enables the investigation of large clusters [20]. On the other side, a significant reordering of minima predicted by empirical potential is observed after re-optimization [21,22] at the DFT level of theory (Density Functional Theory). Although an unbiased GO-DFT investigation appears as more reliable, the quality of the results is also related to the level of approximation on the exchange-correlation energy term within the functional form [23].

Through the example of small  $Pt_n$  clusters ( $n = 6-10$ ) the present work aims at illustrating the sensitivity of the morphological map obtained from GO with respect to the functional form. From the structural investigation of the  $Pt_6$  cluster, the sensitivity of the chemical ordering with the functional form is investigated by using four different classes of functionals: the PBE (Perdew-Burke-Ernzerhof) GGA (Generalized Gradient Approximation) [24], the TPSS (Tao-Perdew-Staroverov-Scuseria) meta-GGA [25] and their respective hybrids (PBE0 [26], TPSSh). The example of the Pt cluster is chosen in reason of its extensive structural investigation in the literature [27–40], mostly performed from first principle calculations at the GGA level. Moreover, the lowest energy structures of  $Pt_{7-10}$  clusters investigated at the TPSSh level are compared with those obtained at the GGA level issuing from the literature.

## 2. Computational details

The  $Pt_n$  cluster structures ( $n = 6, 10$ ) are investigated by the GSAM (Global Search Algorithm of Minima) code [41,42]. In Ref. [41] the method was used for the investigation of the low lying isomers of  $Si_n$  clusters ( $n = 3, 15$ ). The algorithm starts with the generation of an initial set of cartesian coordinates by three generation methods: (i) a simple random generation in 3D space (ii) a random generation in 2D space (iii) a spheroid generation. Similar configurations are then discarded from a topological criterion: each structure is characterized by two geometrical descriptors (nuclear repulsion energy and moments of inertia) and discarded if they differ by less than 0.5% and 3% respectively with another structure. The selected structures are then locally optimized from energy minimization. It is emphasized that the optimization process relies on the so-called “raking optimization” [41]: during  $m$  steps (here  $m = 3$ ), the structures are partially optimized (here 20 cycles of energy minimization per step, i.e. 60 cycles after the 3 steps) and discarded step after step when they appear too high in energy compared to the lowest energy structure at each step. This energetic criterion, initially very coarse, is progressively tightened during the process ( $\Delta E_{m=1} = 4$  eV;  $\Delta E_{m=2} = 2$  eV;  $\Delta E_{m=3} = 1$  eV). Between each successive partial optimization, the topological criterion is applied. Full optimization and frequency computations are then performed for the remaining structures after the third step.

Energy evaluations can be performed from first principle calculations with the Gaussian [43] software. The TPSSh, TPSS, PBE0 and PBE functionals were considered with the use of cc-pVTZpp basis set [44] which also account for the relativistic effect expected to be significant for Pt element (Hartree Fock primitive sets for the valence electrons:  $(10s9p8d2f1g)$  with contractions  $[5s5p4d2f1g]$ ; see Ref. [45] for a complete description). The Def2-SVP basis set [46,47] was also used with the TPSSh functional. The SCF convergence criterion and the maximum number of SCF cycles were set to  $10^{-6}$  and 80, respectively. Moreover the use of a quadratically convergent SCF procedure was specified (keyword SCF=xqc) which allows to turn on the quadratic convergence procedure in case of convergence failure after the 80 cycles. Concerning local optimization, the Berny algorithm [48] was used. Moreover, spin

multiplicities from singlet to nonet were considered for each of the four DFT functionals considered. On that point it is emphasized that no spin contamination is observed (cf. Section 3). Moreover, single point computations were performed at the RMP4(SDQ)/cc-pVTZpp level of theory from the structures obtained at the DFT level.

In total, 25 independent GO were performed for the investigation of  $Pt_6$  from an initial set of 100 generated structures (50 from random 3D generation, 20 from random 2D generation, 30 from spheroidal generation). Concerning the  $Pt_{7-10}$  clusters one GO was performed for each species (a total of 130, 190, 290 and 480 sets of coordinates were generated for  $Pt_7$ ,  $Pt_8$ ,  $Pt_9$ ,  $Pt_{10}$ , respectively) at the TPSSh/Def2SVP level of theory in the quintet spin state. The final structures found in the range [0–1] eV were refined through the GSAM process at the TPSSh/cc-pVTZpp level of theory, considering the five first spin multiplicities.

The computations were performed at the TGCC High Performance Computing center, CEA, France (Supercomputer Curie thin nodes, 5040 nodes, 2 eight-core Intel® processors per node Sandy Bridge EP (E5-2680) 2.7 GHz, 64 GB). 16 cores were used for each Gaussian job (partial local optimization). The jobs were sent simultaneously at each step of the raking optimization.

## 3. Results and discussion

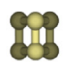
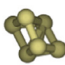

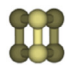
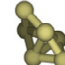
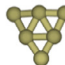
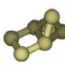


In Table 1 are reported the low-lying minima found for  $Pt_6$  at the PBE, PBE0, TPSS and TPSSh level with the cc-pVTZpp basis set with their corresponding spin multiplicities. The results of TPSSh with the more modest Def2SVP basis set are also reported. Concerning the question of the spin contamination, the values of  $\langle S^2 \rangle - s(s+1)$  does not deviate by more than 0.1 for most of the structures optimized. The maximum deviation before spin projection is below 0.1 for all the structures in quintet, septet and nonet spin states. Concerning the triplet spin state, the deviation can be larger but remains below 10% after annihilation of first spin contaminant, except for the first  $^3Pt_6$  structure at the PBE level ( $\Delta E = 0.44$  eV, not reported in Table 1) exhibiting a deviation of 15%.

Table 1 reveals that planar structures are favored with the use of a pure functional. This is in line with the previous studies: the triangular structure was found as global minimum at the GGA level [27–30,37] with a PAW or atom centered pseudopotential and the double square was found as first isomer [27,30] at about 0.20 eV above the minimum, in agreement with the present study (0.20 eV and 0.33 eV at the PBE and TPSS level, respectively). About the spin multiplicities, the GM triangular structure was found as singlet [30], triplet [37], quintet [28,29] or septet [27] which is consistent with our PBE results that reveal an energetic difference between the four spin states of 0.15 eV ( $3.5 \text{ kcal mol}^{-1}$ ). Moreover the planar double square structure was found triplet [27] or quintet [30], in agreement with our results (about 0.2 eV above the GM for the two spin states at the PBE level). Thus, the previous studies and the results reported in Table 1 reveal that high spin moments can also be observed with the pure functionals for the lowest energy structures.

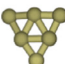
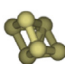
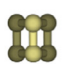
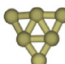
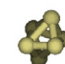

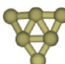


In contrast, the hybrid GGA and hybrid meta-GGA predict that  $Pt_6$  cluster favor the 3D configurations, as reported in Refs. [35,33] from B3LYP [49–52] and B3PW91 [48,53] computations, respectively. Although, according to the Ref. [35], the preference to planar structure could be due to the use of plane waves, the atomic centered basis set used in the present study and those used in the literature with a pure functional [29,37] rather suggests the importance of the functional form. At the PBE0 level, a septet pseudo trigonal prism (PBE0\_6a), a septet pseudo face capped pyramid (PBE0\_6b) and a nonet trigonal prism (PBE0\_6d) are respectively found at 0.00 eV, 0.08 eV and 0.12 eV, in line with

**Table 1**


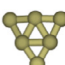

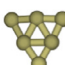
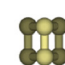
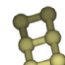

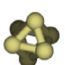

The nine first low lying isomers of Pt<sub>6</sub> with their relative energy ( $\Delta E$  in eV) obtained at different DFT level of theory (PBE, PBE0, TPSS, TPSSH) with the cc-pVTZpp basis set. The numbers in brackets refer to the spin multiplicity. The TPSSH/Def2SVP results are also reported. In *italic*: global minimum reported in the literature: <sup>a</sup>PBE/NAOs [37], <sup>b</sup>B3PW91/LANL2DZ [33], <sup>c</sup>GGA/PAW [30], <sup>d</sup>PW91/ECP(double zeta + polarization) [29], <sup>e</sup>GGA/PAW [28], <sup>f</sup>PW91/PAW [27].

TPSSH/ Def2SVP									
$\Delta E$ (2S+1)	0.00 (7)	0.06 (7)	0.10 (5)	0.15 (9)	0.19 (5)	0.19 (5)	0.23 (3)	0.24 (3)	0.30 (9)

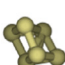


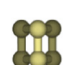
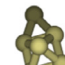

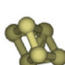

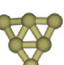
  

TPSSH/ cc-pVTZ-PP									
	6a	6b	6c	6d	6e	6f	6g	6h	6i
$\Delta E$ (2S+1)	0.00 (5)	0.02 (7)	0.02 (9)	0.03 (7)	0.04 (9)	0.14 (7)	0.14 (3)	0.16 (5)	0.16 (5)

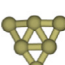
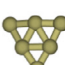

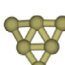
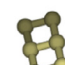
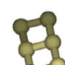
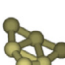

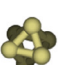
  

TPSS/ cc-pVTZ-PP									
	6a	6b	6c	6d	6e	6f	6g	6h	6i
$\Delta E$ (2S+1)	0.00 (5)	0.06 (3)	0.14 (7)	0.27 (1)	0.32 (9)	0.33 (5)	0.34 (3)	0.34 (9)	0.41 (7)

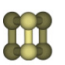
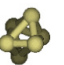
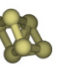
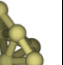
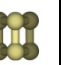
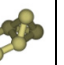
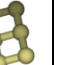
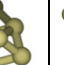
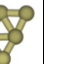
PBE0/ cc-pVTZ-PP									
	6a	7b <i>GM<sup>b</sup></i>	6c	6d	6e	6f	6g	6h	6i
$\Delta E$ (2S+1)	0.00 (7)	0.08 (7)	0.11 (9)	0.12 (9)	0.25 (7)	0.27 (5)	0.30 (5)	0.30 (5)	0.31 (7)

PBE/ cc-pVTZ-PP									
	6a <i>GM<sup>d,c</sup></i>	6b <i>GM<sup>f</sup></i>	6c <i>GM<sup>f</sup></i>	6d <i>GM<sup>f</sup></i>	6e	6f	6g	6h	6i
$\Delta E$ (2S+1)	0.00 (5)	0.01 (3)	0.15 (7)	0.16 (1)	0.20 (5)	0.21 (3)	0.39 (7)	0.54 (7)	0.68 (9)

**Table 2**

Qualitative chemical ordering (in eV) of the Pt<sub>6</sub> structures reported in Fig. 1 from single point calculations at the ROMP4/cc-pVTZpp level theory. The numbers in brackets refer to the spin multiplicity.

ROMP4 <sup>SP</sup> / cc-pVTZ-PP									
$\Delta E$ (2S+1)	0.00 (9)	0.51 (9)	0.74 (7)	0.82 (5)	0.91 (7)	0.93 (3)	1.02 (5)	1.27 (3)	1.29 (3)

the B3LYP computations [35] (0.00 eV, 0.15 eV, 0.17 eV for a septet trigonal prism, a septet face capped pyramid and a nonet trigonal prism, respectively) and the B3PW91 results [33] which described PBE0\_6b as GM. The relative positions of the quintet pseudo face capped pyramid (PBE0\_6g) and the septet triangle structure (PBE0\_6i) (0.30 eV and 0.31 eV) are also in agreement with Ref. [35] (0.25 and 0.39 eV). The same trend is observed from the TPSSH computations, even with the more modest Def2SVP basis set, although triangular structure appears as favored as 3D structures with the larger cc-pVTZ-PP basis set. Concerning the effect of the spin-orbit coupling, it has been found that 3D configurations are still favored at the B3LYP level [35] and noticed that the relative

stability of Pt clusters is not affected with the inclusion of spin-orbit effect [27].

From Table 1, the study reveals that triplet and quintet spin states for planar structures are favored with the pure functional while septet and nonet spin states for 3D structures are obtained with the use of their hybrid counterparts. A comparison with experimental measured magnetic moments [54] would be desirable to classify the two situations, nevertheless a conclusion can be drawn from further calculations at higher level of theory. On that point, single point energies for the ten most pertinent atomic arrangements issuing from DFT computations (see Fig. 1) were performed at the (RO)MP4 (SDQ) level of theory for each of the first

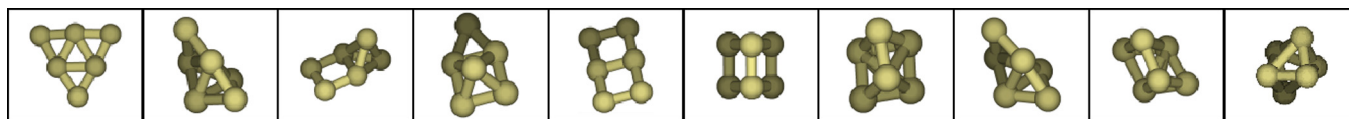
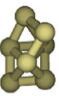
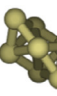
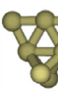
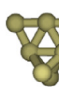
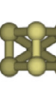
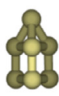
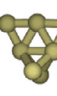
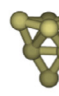
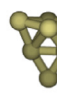

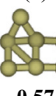
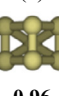

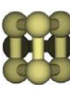
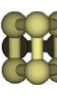


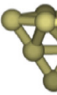
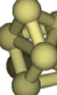
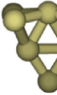
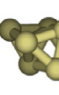

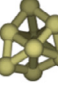
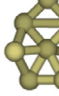
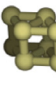
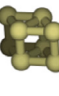
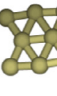
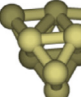
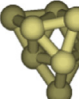
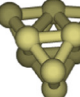
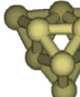
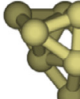
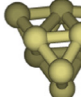
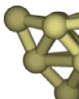

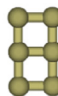
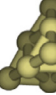
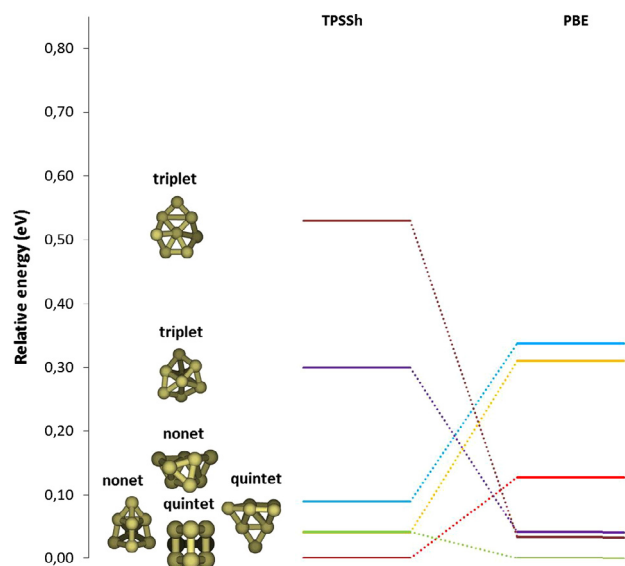


Table 3

Low lying isomers of Pt<sub>7</sub>, Pt<sub>8</sub>, Pt<sub>9</sub> with their relative energy in bold ( $\Delta E$  in eV) obtained at the TPSSH/cc-pVTzp level of theory. The numbers in brackets refer to the spin multiplicity. In italic: global minimum reported in the literature: <sup>a</sup>PBE/NAOS[37], <sup>b</sup>B3PW91/LANL2DZ[33], <sup>c</sup>GGA/PAW[30], <sup>d</sup>PW91/ECP(double zeta + polarization)[29], <sup>e</sup>GGA/PAW[28], <sup>f</sup>PW91/PAW[27], <sup>g</sup>PW91/LANL2DZ[36]. The GM of Pt<sub>10</sub> is also reported.

Pt <sub>7</sub>								
								
7a <b>0.00</b> (5)	7b <b>0.02</b> (9)	7c <i>GM</i> <sup>a</sup> <b>0.07</b> (5)	7d <b>0.09</b> (7)	7e <b>0.15</b> (5)	7f <b>0.16</b> (5)	7g <b>0.17</b> (3)	7h <b>0.18</b> (7)	7i <b>0.20</b> (5)
...								
			<b>0.35</b> (3) <i>GM</i> <sup>b,f</sup>	<b>0.57</b> (5) <i>GM</i> <sup>c</sup>	<b>0.96</b> (1) <i>GM</i> <sup>d</sup>	<b>&gt;1.00</b> (1) <i>GM</i> <sup>e</sup>		
Pt <sub>8</sub>								
								
8a <b>0.00</b> (5)	8b <b>0.03</b> (3)	8c <b>0.04</b> (9)	8d <b>0.04</b> (7)	8e <b>0.04</b> (5)	8f <b>0.05</b> (9)	8g <b>0.06</b> (5)	8h <b>0.09</b> (9)	8i <b>0.14</b> (3)
...								
		<b>0.30</b> (3) <i>GM</i> <sup>c,g</sup>	<b>0.53</b> (3) <i>GM</i> <sup>a</sup>	<b>0.60</b> (9) <i>GM</i> <sup>b</sup>	<b>0.66</b> (7) <i>GM</i> <sup>f</sup>	<b>&gt;1.00</b> (3) <i>GM</i> <sup>e</sup>		
Pt <sub>9</sub>								
								
9a <b>0.00</b> (7)	9b <b>0.04</b> (9)	9c <b>0.09</b> (5)	9d <b>0.10</b> (9)	9e <b>0.12</b> (7)	9f <b>0.17</b> (3)	9g <b>0.18</b> (5)		
...								
		<b>0.58</b> (7) <i>GM</i> <sup>b,d,f</sup>	<b>&gt;1.00</b> (5) <i>GM</i> <sup>a,c</sup>					
Pt <sub>10</sub>								
								
10a <b>0.00</b> (9) <i>GM</i> <sup>a,c,e</sup>								





**Fig. 2.** Sensitivity of low-lying planar and 3D compact  $Pt_8$  structures with respect to the functional. The relative energies at the PBE/cc-pVTZpp level of theory were obtained from the re-optimization of the TPSSH/cc-pVTZpp structures found from Global Optimizations.

five spin states. A Restricted Open shell scheme was chosen in reason of large spin contamination observed for the UHF (Unrestricted Hartree-Fock) wavefunctions. The results are reported in Table 2 and show that the septet and nonet 3D structures are favored. We point out the qualitative picture provided by the results in reason of the convergence behavior of a MPn series. Anyway, the results point in a direction that suggests a more correct description of the electronic structure of Pt clusters at the DFT level of theory with the use of hybrid functionals.

Table 3 reports the low lying energy structures of  $Pt_7$ ,  $Pt_8$  and  $Pt_9$  clusters investigated at the TPSSH/cc-pVTZpp level of theory for the first five spin states. The structures are issuing from a re-optimization of the quintet spin state structures found in the range [0–1 eV] by preliminary Global Optimizations at the TPSSH/Def2SVP level of theory. Among the  $Pt_n$  morphologies reported as low energy structures (from  $n_a$  to  $n_i$  in Table 3) only four were found in the literature: the  ${}^5Pt_{7a}$ , considered as two fused square pyramids, the double face capped pyramid  ${}^9Pt_{7b}$ , the atom capped triangle  ${}^5Pt_{7c}$  and the face capped trigonal prism  ${}^5Pt_{7f}$  were found with a GGA functional as second isomer in Ref. [30], second isomer in Ref. [27], GM in Ref. [37] and first isomer in Ref. [28], respectively. The GM found in the literature (see Table 3), and more particularly the planar structures, are higher in energy at the TPSSH level. As shown in Fig. 2, which reports from Table 3 the relative energy of some low lying planar and 3D compact  $Pt_8$  structures optimized both at the TPSSH and PBE level, the 3D compact structures we found are particularly disfavored at the PBE level: all the 3D TPSSH structures considered in Fig. 2. ( ${}^5Pt_{8a}$ ,  ${}^9Pt_{8c}$ ,  ${}^9Pt_{8h}$ ) appears as highest energy structures in the PBE picture. The triplet and the quintet quasi-planar structures are in turn lowered and take place in the energy range of GM as reported in Refs. [30,36,37] for the triplet spin state species. Nevertheless, whichever the functional used, the lowest energy of  $Pt_{10}$  cluster adopts for most of the investigations [28,30,37] the nonet three-dimensional stacked pyramid structure as shown in Table 3. On that point the picture depicted by the TPSSH functional reveals a growth pattern from  $Pt_6$  to  $Pt_{10}$  in which the three-dimensional stacked pyramid could be built from successive additions of one Pt atom implying lower morphological perturbations through lowest energy structures. Thus, and considering the qualitative trend reported in Table 2, the use of a

hybrid functional seems preferable for a more correct description of the electronic structure of Pt clusters at the DFT level.

#### 4. Conclusion

The chemical ordering of  $Pt_6$  structures were investigated with four classes of functionals: GGA (PBE), hybrid GGA (PBE0), meta-GGA (TPSS) and hybrid meta-GGA (TPSSH), with the cc-pVTZpp basis set. Moreover, the spin multiplicities from singlet to nonet were considered. The results yielded two different pictures: singlet to septet planar structures are favored with the pure functionals while quintet to nonet 3D structures appear as the lowest energy structures or first isomers with their hybrid counterpart. Qualitative trends obtained from single point RMP4(SDQ) calculations on the optimized DFT structures suggested a more correct description at the DFT level by the use of hybrid functionals. The investigation of the lowest energy structures of  $Pt_{7-10}$  clusters at the TPSSH level in comparison with the GGA picture issuing from the literature confirm the preference for 3D compact structures. This highlights a different morphological map of the small  $Pt_n$  clusters and suggests a clearer pattern growth from  $Pt_6$  toward the lowest energy  $Pt_{10}$  structure.

#### Acknowledgements

Computer time for this study was provided by the computing facilities of the MCIA (Mésocentre de Calcul Intensif Aquitain) of the Université de Bordeaux and of the Université de Pau et des Pays de l'Adour, and the TGCC (Très Grand Centre de Calcul du CEA), Bruyères-Le-Châtel (Essonne), France. This work was supported by the CNRS (Centre National de la Recherche Scientifique) and the CG64 (Conseil Général des Pyrénées Atlantiques) for the PhD funding of R. Li. The COST action MOLIM CM 1405 is also acknowledged.

#### References

- [1] E.E. Finney, R.G. Finke, Nanocluster nucleation and growth kinetic and mechanistic studies: a review emphasizing transition-metal nanoclusters, *J. Colloid Interf. Sci.* 317 (2008) 351–374.
- [2] E.J. Yoo, T. Okada, T. Akita, M. Kohyama, I. Honma, J. Nakamura, Sub-nano-Pt cluster supported on graphene nanosheets for CO tolerant catalysts in polymer electrolyte fuel cells, *J. Power Sources* 196 (2011) 110–115.
- [3] F. Calvo, Non-genetic global optimization methods in molecular sciences: An overview, *Comput. Mater. Sci.* 45 (2009) 8–15.
- [4] D.J. Wales, A.S. Harold, Global optimization of clusters, crystals and biomolecules, *Science* 285 (1999) 1368–1372.
- [5] B. Hartke, Global optimization, *Wiley Interdiscipl. Rev. Comput. Mol. Sci.* 1 (2011) 879–887.
- [6] S. Heiles, R.L. Johnston, Global optimization of clusters using electronic structure methods, *Int. J. Quantum Chem.* 113 (2013) 2091–2109.
- [7] M. Iwamatsu, Global geometry optimization of silicon clusters using the space-fixed genetic algorithm, *J. Chem. Phys.* 112 (2000) 10976.
- [8] L. Pedroza, A.J. da Silva, Ab initio Monte Carlo simulation applied to a Si5 cluster, *Phys. Rev. B* 75 (2007) 245331.
- [9] S. Kirkpatrick, C.D. Gelatt, M.P. Vecchi, Optimization by simulated annealing, *Science* 220 (1983) 671–680.
- [10] D.J. Earl, M.W. Deem, Parallel tempering: theory, applications, and new perspectives, *Phys. Chem. Chem. Phys.* 7 (2005) 3910–3916.
- [11] R.L. Johnston, Evolving better nanoparticles: genetic algorithms for optimizing cluster geometries, *Dalton Trans.* 22 (2003) 41934207.
- [12] D.J. Wales, J.P.K. Doye, Global optimization by Basin-Hopping and the lowest energy structures of Lennard-Jones clusters containing up to 110 atoms, *J. Phys. Chem. A* 101 (1997) 5111–5116.
- [13] N. Issaoui, K. Abdessalem, H. Ghalla, S.J. Yaghmour, F. Calvo, B. Oujia, Theoretical investigation of the relative stability of  $Na^+He_n$  ( $n = 2-24$ ) clusters: many-body versus delocalization effects, *J. Chem. Phys.* 141 (2014) 174316.
- [14] M. Born, J.E. Mayer, Zur gittertheorie der ionenkristalle, *Zeitschrift Physik* 75 (1932) 1–18.
- [15] J.E. Jones, On the determination of molecular fields. II. From the equation of state of a gas, *Proc. R. Soc. Lond. Ser. A* 106 (1924) 463–477.
- [16] P.M. Morse, Diatomic molecules according to the wave mechanics. II. Vibrational levels, *Phys. Rev.* 34 (1929) 57.

- [17] J.P. Doye, D.J. Wales, F.H. Zetterling, M. Dzugutov, The favored cluster structures of model glass formers, *J. Chem. Phys.* 118 (2003) 2792–2799.
- [18] A.P. Sutton, J. Chen, Long-range Finnis-Sinclair potentials, *Philos. Mag. Lett.* 61 (1990) 139–146.
- [19] R.P. Gupta, Lattice relaxation at a metal surface, *Phys. Rev. B* 23 (1981) 6265–6270.
- [20] D. Boichichio, R. Ferrando, R. Novakovic, E. Panizon, G. Rossi, Chemical ordering in magic-size Ag-Pd nanoparticles, *Phys. Chem. Chem. Phys.* 16 (2014) 26478–26484.
- [21] J.B.A. Davis, R.L. Johnston, L. Rubinovich, M. Polak, Comparative modelling of chemical ordering in palladium-iridium nanoalloys, *J. Chem. Phys.* 141 (2014) 224307.
- [22] D.D.C. Rodriguez, A.M. Nascimento, H.A. Duarte, J.C. Belchior, Global optimization analysis of CunAum (n+m=38) cluster: Complementary ab initio calculations, *Chem. Phys.* 349 (2008) 91–97.
- [23] R. Car, Fixing Jacob's ladder, *Nature Chem.* 8 (2016) 820–821.
- [24] J.P. Perdew, K. Burke, M. Ernzerhof, Generalized gradient approximation made simple, *Phys. Rev. Lett.* 77 (1996) 3865–3868.
- [25] J.M. Tao, J.P. Perdew, V.N. Staroverov, G.E. Scuseria, Climbing the density functional ladder: Nonempirical meta-generalized gradient approximation designed for molecules and solids, *Phys. Rev. Lett.* 91 (2003) 146401.
- [26] C. Adamo, V. Barone, Toward reliable density functional methods without adjustable parameters: the PBE0 model, *J. Chem. Phys.* 110 (1999) 6158–6169.
- [27] L. Xiao, L.C. Wang, Structures of platinum clusters: Planar or spherical?, *J. Phys. Chem. A* 108 (2004) 8605–8614.
- [28] K. Bhattacharyya, C. Majumder, Growth pattern and bonding trends in Ptn (n = 2–13) clusters: theoretical investigation based on first principle calculations, *Chem. Phys. Lett.* 446 (2007) 374–379.
- [29] A.H. Nie, J.P. Wu, C.G. Zhou, S.J. Yao, C. Luo, R.C. Forrey, H.S. Cheng, Structural evolution of subnano platinum clusters, *Int. J. Quantum Chem.* 107 (2007) 219–224.
- [30] V. Kumar, Y. Kawazoe, Evolution of atomic and electronic structure of Pt clusters: planar, layered, pyramidal, cage, cubic, and octahedral growth, *Phys. Rev. B* 77 (2008) 205418.
- [31] X.L. Wang, D.X. Tian, Structures and structural evolution of Ptn (n = 15–24) clusters with combined density functional and genetic algorithm methods, *Comput. Mater. Sci.* 46 (2009) 239–244.
- [32] H.K. Yuan, H. Chen, A.L. Kuang, B. Wu, Spin-orbit effect and magnetic anisotropy in Pt clusters, *J. Magn. Mater.* 331 (2013) 7–16.
- [33] C.L. Heredia, V. Ferraresi-Curotto, M.B. López, Characterization of Ptn (n = 2–12) clusters through global reactivity descriptors and vibrational spectroscopy, a theoretical study, *Comput. Mater. Sci.* 53 (2012) 18–24.
- [34] A. Sebetci, Z.B. Güvenç, Energetics and structures of small clusters: Ptn, n = 2–21, *Surf. Sci.* 525 (2003) 66–84.
- [35] A. Sebetci, Does spin-orbit coupling effect favor planar structures for small platinum clusters?, *Phys. Chem. Chem. Phys.* 11 (2009) 921–925.
- [36] A. Sebetci, New minima for the Pts cluster, *Comput. Mater. Sci.* 78 (2013) 9–11.
- [37] A.S. Chaves, G.G. Rondina, M.J. Piotrowski, P. Tereshchuk, J.L.F. Da Silva, The role of charge states in the atomic structure of Cun and Ptn (n = 2–14 atoms) clusters: A DFT investigation, *J. Phys. Chem. A* 118 (2014) 10813–10821.
- [38] B. Hamad, Z. El-Bayyari, A. Marashdeh, Investigation of the stability of platinum clusters and the adsorption of nitrogen monoxide: first principles calculations, *Chem. Phys.* 443 (2014) 26–32.
- [39] D.J. Harding, C. Kerpel, D.M. Rayner, A. Fielicke, Communication: the structures of small cationic gas-phase platinum clusters, *J. Chem. Phys.* 136 (2012) 211103.
- [40] P.G. Alvarado-Leyva, F. Aguilera-Granja, A. Garcia-Fuente, A. Vega, Spin-orbit effects on the structural, homotop, and magnetic configurations of small pure and Fe-doped Pt clusters, *J. Nanopart. Res.* 16 (2014) 2222.
- [41] R. Marchal, P. Carbonnière, C. Pouchan, A global search algorithm of minima exploration for the investigation of low lying isomers of clusters from density functional theory-based potential energy surfaces: the example of Sin (n = 3,15) as test case, *J. Chem. Phys.* 131 (2009) 114105.
- [42] R. Marchal, G. Manca, S. Kahlal, P. Carbonnière, C. Pouchan, J.-F. Halet, J.-Y. Saillard, Structures and stabilities of small, ligated AlnLn0/2– and AlnLn+2 clusters (L = H, Cl) – A theoretical study, *Eur. J. Inorg. Chem.* 30 (2012) 4856–4866.
- [43] M.J. Frisch, G.W. Trucks, H.B. Schlegel, G.E. Scuseria, M.A. Robb, J.R. Cheeseman, G. Scalmani, V. Barone, B. Mennucci, G.A. Petersson, et al., Gaussian 09, Gaussian Inc., Wallingford, CT, USA, 2009.
- [44] D. Figgen, K.A. Peterson, M. Dolg, H. Stoll, Energy-consistent pseudopotentials and correlation consistent basis sets for the 5d elements Hf–Pt, *J. Chem. Phys.* 130 (2009) 164108.
- [45] <https://bse.pnl.gov/bse/portal>.
- [46] F. Weigend, R. Ahlrichs, Balanced basis sets of split valence, triple zeta valence and quadruple zeta valence quality for H to Rn: design and assessment of accuracy, *Phys. Chem. Chem. Phys.* 7 (2005) 3297–3305.
- [47] F. Weigend, Accurate Coulomb-fitting basis sets for H to Rn, *Phys. Chem. Chem. Phys.* 8 (2006) 1057–1065.
- [48] H.B. Schlegel, Optimization of equilibrium geometries and transition structures, *J. Comput. Chem.* 3 (1982) 214–218.
- [49] A.D. Becke, Density-functional thermochemistry. III. The role of exact exchange, *J. Chem. Phys.* 98 (1993) 5648–5652.
- [50] C. Lee, W. Yang, R.G. Parr, Development of the Colle-Salvetti correlation-energy formula into a functional of the electron density, *Phys. Rev. B* 37 (1988) 785–789.
- [51] S.H. Vosko, L. Wilk, M. Nusair, Accurate spin-dependent electron liquid correlation energies for local spin density calculations: a critical analysis, *Can. J. Phys.* 58 (1980) 1200–1211.
- [52] P.J. Stephens, F.J. Devlin, C.F. Chabalowski, M.J. Frisch, Ab initio calculation of vibrational absorption and circular dichroism spectra using density functional theory, *J. Phys. Chem.* 98 (1994), 11623–1162.
- [53] J.P. Perdew, J.A. Chevary, S.H. Vosko, K.A. Jackson, M.R. Pederson, D.J. Singh, C. Fiolhais, Atoms, molecules, solids, and surfaces: applications of the generalized gradient approximation for exchange and correlation, *Phys. Rev. B* 46 (1992) 6671–6687.
- [54] A.M. Koster, P. Calaminici, E. Orgaz, D.R. Roy, J.U. Reveles, S.N. Khanna, On the ground state of Pd13, *J. Am. Chem. Soc.* 133 (2011) 12192–12196.